THE JOURNAL OF BIOLOGICAL CHEMISTRY VOL. 289, NO. 41, pp. 28237–28248, October 10, 2014

Diacylglycerol Acyltransferase-2 (DGAT2) and Monoacylglycerol Acyltransferase-2 (MGAT2) Interact to Promote Triacylglycerol Synthesis*

Received for publication, April 3, 2014, and in revised form, August 13, 2014 Published, JBC Papers in Press, August 27, 2014, DOI 10.1074/jbc.M114.571190

Youzhi Jin[‡1], **Pamela J. McFie**[‡1], **Shanna L. Banman**[§], **Curtis Brandt**[‡], **and Scot J. Stone**[‡2]

From the [‡]*Department of Biochemistry, University of Saskatchewan, Saskatoon, Saskatchewan S7N 5E5, Canada and* [§]*Western College of Veterinary Medicine, University of Saskatchewan, Saskatoon, Saskatchewan S7N 5B4, Canada*

Background: DGAT2 catalyzes the final and committed step of triacylglycerol (TG) biosynthesis.
Results: Co-immunoprecipitation experiments and *in situ* proximity ligation assays showed that DGAT2 and MGAT2 interact.
Conclusion: DGAT2 can utilize diacylglycerol generated by MGAT2 for TG synthesis.
Significance: These findings provide insight into the spatial arrangement of enzymes involved in triacylglycerol biosynthesis.

Acyl CoA:1,2-diacylglycerol acyltransferase (DGAT)-2 is an integral membrane protein that catalyzes triacylglycerol (TG) synthesis using diacylglycerol and fatty acyl CoA as substrates. DGAT2 resides in the endoplasmic reticulum (ER), but when cells are incubated with fatty acids, DGAT2 interacts with lipid droplets presumably to catalyze localized TG synthesis for lipid droplet expansion. Previous studies have shown that DGAT2 interacts with proteins that synthesize its fatty acyl CoA substrates. In this study, we provide additional evidence that DGAT2 is present in a protein complex. Using a chemical cross-linker, disuccinimidyl suberate (DSS), we demonstrated that DGAT2 formed a dimer and was also part of a protein complex of ~650 kDa, both in membranes and on lipid droplets. Using co-immunoprecipitation experiments and an *in situ* proximity ligation assay, we found that DGAT2 interacted with monoacylglycerol acyltransferase (MGAT)-2, an enzyme that catalyzes the synthesis of diacylglycerol. Deletion mutagenesis showed that the interaction with MGAT2 was dependent on the two transmembrane domains of DGAT2. No significant interaction of DGAT2 with lipin1, another enzyme that synthesizes diacylglycerol, could be detected. When co-expressed in cells, DGAT2 and MGAT2 co-localized in the ER and on lipid droplets. Co-expression also resulted in increased TG storage compared with expression of DGAT2 or MGAT2 alone. Incubating McArdle rat hepatoma RH7777 cells with 2-monoacylglycerol caused DGAT2 to translocate to lipid droplets. This also led to the formation of large cytosolic lipid droplets, characteristic of DGAT2, but not DGAT1, and indicated that DGAT2 can utilize monoacylglycerol-derived diacylglycerol. These findings suggest that the interaction of DGAT2 and MGAT2 serves to channel lipid substrates efficiently for TG biosynthesis.

Diacylglycerol acyltransferase (DGAT)[3]-2 catalyzes the formation of an ester bond between an activated fatty acid (fatty acyl CoA) and 1,2-diacylglycerol producing triacylglycerol (TG) (1, 2). TG is the major stored form of energy in most organisms and is sequestered in the hydrophobic core of cytosolic lipid droplets until it is needed (3). Lipid droplets are believed to originate at the endoplasmic reticulum (ER), where most of the enzymes involved in TG synthesis are thought to reside. An energy surplus within cells also promotes the growth of existing lipid droplets, which is thought to occur by expansion events requiring localized TG synthesis and/or by coalescence of smaller droplets to form larger ones.

DGAT2 belongs to an evolutionarily conserved acyltransferase gene family and is highly expressed in tissues that have a robust capacity for TG synthesis and storage (adipose tissue, liver, small intestine, and mammary gland) (1, 4, 5). All DGAT2 family members, including monoacylglycerol acyltransferases (MGAT) 1–3 and wax synthases 1 and 2, contain a highly conserved four amino acid sequence - histidine-proline-histidine-glycine (4, 5). Mutagenesis of amino acids within this sequence, in particular the two histidine residues, markedly impaired the catalytic function of DGAT2 and suggested that this region is part of the active site (6). DGAT2 also contains several other highly conserved regions. However, their functional importance has yet to be determined (5).

DGAT2 appears to be involved in promoting bulk TG synthesis. Expression of DGAT2 in hepatoma cells or mouse liver resulted in large increases in intracellular TG stored in cytosolic lipid droplets (7, 8). In contrast, mice lacking DGAT2 have almost no TG and die shortly after birth (8).

DGAT2 is an integral membrane protein that contains two transmembrane domains with both its N- and C termini exposed to the cytosol (6). Although present in ER membranes, incubating cells with fatty acids causes DGAT2 to associate

* This work was supported in part by a Heart and Stroke Foundation of Saskatchewan Grant-in-Aid, CIHR (FRN 123385) and the CFI.
[1] Both authors contributed equally to this work.
[2] To whom correspondence should be addressed: Dept. of Biochemistry, University of Saskatchewan, 107 Wiggins Rd., Saskatoon, Saskatchewan S7N 5E5, Canada. Tel.: 306-966-4217; Fax: 306-966-4390; E-mail: scot.stone@usask.ca.

[3] The abbreviations used are: DGAT, acyl CoA: 1,2-diacylglycerol acyltransferase; ADRP, adipose differentiation-related protein; CE, cholesterol ester; DG, 1,2-diacylglycerol; DSS, disuccinimidyl suberate; ER, endoplasmic reticulum; FATP, fatty acid transport protein; HSP70, heat shock protein 70; MGAT, acyl CoA:2-monoacylglycerol acyltransferase; NBD, *N*-[(7-nitro-2–1,3-benzoxadiazol-4-yl)-methyl]amino; SCD, stearoyl CoA desaturase; TG, triacylglycerol.

with lipid droplets where it can catalyze TG synthesis for lipid droplet expansion (9–11). Isolated lipid droplets, containing DGAT2, were found to be capable of catalyzing TG synthesis in an *in vitro* assay when exogenous diacylglycerol was provided (11). However, the source of diacylglycerol for TG synthesis on lipid droplets in intact cells has not been determined.

Diacylglycerol can be synthesized through two distinct pathways. In the Kennedy pathway, phosphatidate formed from the acylation of glycerol-3-phosphate is dephosphorylated by phosphatidate phosphatase producing 1,2-diacylglycerol (2). This diacylglycerol can then be used as a substrate by DGAT enzymes to synthesize TG or incorporated into phospholipids. The identity of the gene encoding phosphatidate phosphatase has only recently been identified (12). Lipin, which had an established role as a transcriptional co-regulator of liver fatty acid oxidation and adipogenesis has now also been shown to function as a phosphatidate phosphatase (12, 13).

In the intestine, the majority of diacylglycerol is produced by the MGAT pathway via MGAT2, one of several related DGAT2/MGAT enzymes (14, 15). In an analogous reaction to that catalyzed by DGAT, MGAT2 catalyzes the synthesis of diacylglycerol in an acyl CoA-dependent manner using 2-monoacylglycerol as an acyl acceptor (16, 17). This diacylglycerol can then be used by DGAT enzymes to re-synthesize dietary TG in enterocytes. This pathway is important for the absorption and transport of dietary TG from the intestine to other tissues through the circulation via chylomicrons. Interestingly, MGAT2 is also expressed at high levels in human liver, indicating that the MGAT pathway of TG biosynthesis likely has an underappreciated role in this tissue as well (15).

In this study, we show that DGAT2 is part of a large protein complex both in membranes and on lipid droplets. We also show that DGAT2 interacts with MGAT2. Presumably, the interaction with MGAT2 serves to channel diacylglycerol to DGAT2, where it can be esterified to produce TG in an efficient manner.

EXPERIMENTAL PROCEDURES

Cell Culture—COS-7 and HEK-293T cells (American Type Culture Collection) were cultured in Dulbecco's modified Eagle's medium (DMEM) with 10% fetal bovine serum in a 37 °C incubator with 5% CO_2 unless otherwise indicated. McArdle rat hepatoma RH7777 cells (American Type Culture Collection) were cultured in DMEM with 10% fetal bovine serum and 10% horse serum in a 37 °C incubator with 5% CO_2.

Lipid droplet formation was stimulated by incubating cells with 0.5 mM oleate complexed to 0.67% fatty acid-free bovine serum albumin. For some experiments, lipid droplet formation was stimulated by incubating cells with 2-monoacylglycerol (MG). *sn*-2-monoolein (Santa Cruz Biotechnology) was dissolved in 0.5% ethanol (*v*/final volume) and then dispersed in DMEM containing 100 μM fatty acid-free bovine serum albumin (18). The mixture was then incubated at 37 °C for 1 h with shaking and then incubated with cells.

Cell Transfection—20 μg of plasmid DNA was incubated with 430 μl of 0.15 M NaCl and 120 μl of 0.1% polyethylenimine (pH 7.0) for 10 min at room temperature. The transfection mixture was then added dropwise to a 100-mm culture dish with cells (HEK-293T, COS-7, or McArdle RH7777) at ~50% confluency containing 10 ml of DMEM with 10% fetal bovine serum. After 4 h, the transfection solution was removed, and cells were washed and re-fed with fresh media. 24–48 h after transfection, cells were used for experiments.

Generation of DGAT2 Mutants—Mutations were introduced into cDNA sequences by PCR using PfuUltra DNA polymerase (Stratagene). All plasmids were sequenced to confirm the presence of the desired mutations.

Chemical Cross-linking—For *in vitro* cross-linking, total cellular membranes (1 μg/μl protein) were resuspended in 10 mM Hepes (pH 7.4)/1 mM EDTA and were incubated with disuccinimidyl suberate (DSS) (Pierce) at the indicated concentrations. DSS was dissolved in DMSO (2.5% (final)). Reactions were allowed to proceed for 30 min at room temperature and were then terminated by the addition of 1/10 volume of 1 M Tris-Cl (pH 8.0). Samples were separated by SDS-PAGE and analyzed by immunoblotting with anti-FLAG (Sigma).

Cross-linking Intact Cells—Transfected HEK-293T cells were incubated with 500 μM DSS (dissolved in DMSO) for 30 min. Reactions were quenched with 1 M Tris-Cl (pH 7.4). Cells were then harvested and used for the experiments described in the figure legends.

Immunofluorescence Microscopy—24 h after transfection, cells were re-plated into 6-well dishes containing glass coverslips and allowed to adhere overnight. Cells were fixed with 4% paraformaldehyde in phosphate-buffered saline (PBS) for 10 min followed by permeabilization of cellular membranes with 0.2% Triton X-100 for 2 min. Cells were washed with PBS and incubated with 3% bovine serum albumin in PBS for 5 min to block nonspecific antibody binding. Cells were incubated for 1 h with either mouse anti-FLAG (1:500 dilution) and rabbit anti-DGAT2 (1:300 dilution) and then with donkey anti-mouse 594 (Invitrogen; 1:200 dilution) and goat anti-rabbit Alexa Fluor 488 (Invitrogen; 1:200 dilution) secondary antibodies for 30 min at room temperature. In some experiments, lipid droplets were visualized by staining fixed cells with BODIPY 493/503 (Invitrogen). Cells were washed three times with PBS, and the coverslips were mounted on glass slides with a drop of Immuno-Fluore mounting medium (ICN). Confocal images were acquired using a Leica SP5 laser-scanning confocal microscope.

Isolation of Membrane Fractions and Floating Fat Layer—Cells were washed twice with ice-cold PBS, harvested by scraping, and collected by centrifugation (600 × *g*). Cells were resuspended in PBS and disrupted by 15 passages through a 27-gauge needle. Cell debris and nuclei were pelleted by centrifugation at 1,000 × *g* for 5 min. The supernatant was centrifuged at 10,000 × *g* for 10 min at 4 °C to pellet crude mitochondria (mitochondria and mitochondrial-associated membranes), which were resuspended in 50 mM Tris-Cl (pH 7.6)/250 mM sucrose. The supernatant was centrifuged at 100,000 × *g* for 30 min at 4 °C to pellet microsomes, which were resuspended in 50 mM Tris-Cl (pH 7.6)/250 mM sucrose.

To isolate the floating fat layer, the 10,000 × *g* supernatant from above was adjusted to 20% sucrose and overlaid onto 1 ml of 60% sucrose in 20 mM Tris-Cl (pH 7.4)/1 mM EDTA. 6 ml of 5% sucrose in the same buffer was then added, and the tube was

filled to the top with ~5 ml 20 mM Tris-Cl (pH 7.4)/1 mM EDTA. The tube was centrifuged at 200,000 × *g* for 30 min at 4 °C (SW40 rotor). The fat layer at the top of the tube was removed to a 1.5 ml tube and diluted with 20 mM Tris-Cl (pH 7.4)/1 mM EDTA.

In Vitro MGAT Assay—MGAT activity was determined by measuring the formation of *N*-[(7-nitro-2–1,3-benzoxadiazol-4-yl)-methyl]amino (NBD)-DG from NBD-palmitoyl-CoA (19). The reaction mixture consisted of 100 mM Tris-Cl (pH 7.5), 20 mM $MgCl_2$, 0.625 mg/ml BSA, 200 μM 2-monooleoylglycerol, 25 μM NBD-palmitoyl-CoA (Avanti Polar Lipids), and 100 μg of protein sample, in a final volume of 200 μl. Samples were incubated at 37 °C for 10 min, and reactions were terminated by the addition of chloroform:methanol (2:1). Lipids were extracted and separated by thin layer chromatography in diethyl ether/hexane/methanol/acetic acid (55:45:5:1). NBD-DG was detected with a VersaDoc 4000 molecular imaging system (Bio-Rad), and fluorescence was quantified with Quantity One software (Bio-Rad).

Lipid Analyses—Lipids were extracted from cell lysates by the method of Bligh and Dyer (20) with $ClCH_3$:MeOH (2:1) and separated by thin layer chromatography on silica gel G-60 thin layer chromatography plates in the solvent hexane:diethyl ether:acetic acid (80:20:1). Lipids were visualized by charring the thin layer plate with 10% cupric sulfate and 8% phosphoric acid and heating at 180 °C for ~10 min. Lipid levels were quantified using Quantity One image analysis software (Bio-Rad).

Co-immunoprecipitation—HEK-293T or McArdle RH7777 cells were co-transfected with FLAG-DGAT2 (FL-DGAT2) and myc-MGAT2 (Origene) plasmid DNA. 48 h post-transfection, cells were solubilized with 400 μl of 0.5% CHAPS detergent in PBS. Insoluble material was removed by centrifugation, and the solubilized material was transferred to a fresh tube. A 20-μl aliquot (5% of the total) was removed to determine expression levels (input). Samples were then incubated with 30 μl of anti-FLAG agarose beads and rotated for 3 h. Control experiments were performed using an irrelevant mouse antibody and protein A agarose beads. Beads were washed with 0.5% CHAPS in PBS, and bound proteins were eluted with 50 μl of 0.5% CHAPS in PBS containing 150 ng/μl FLAG peptide. A 6-μl aliquot of the immunoprecipitates were analyzed by immunoblotting with anti-FLAG and anti-myc antibodies. All manipulations were performed at 4 °C.

Reciprocal immunoprecipitation experiments were performed as described above with the following modifications. HEK-293T cells were co-transfected with FLAG-MGAT2 (FL-MGAT2) and myc-DGAT2 or untagged DGAT2 cDNAs. FL-MGAT2 was immunoprecipitated using anti-FLAG agarose beads. Immunoprecipitates were then analyzed by immunoblotting with anti-FLAG and anti-DGAT2 antibodies.

For some co-immunoprecipitation experiments, HEK-293T cells were co-transfected with Myc-DGAT1 or Myc-DGAT2 and FLAG-lipin1 (FL-lipin1) (21) (from D. Sabatini, Whitehead Institute for Biomedical Research, Cambridge, MA (Addgene 32005)).

Proximity Ligation Assay—COS-7 cells expressing FL-DGAT2 and/or myc-MGAT2 were incubated with 0.5 mM oleate for 18 h. Cells were fixed and permeabilized as described for immunofluorescence microscopy. Cells were then incubated for 30 min with mouse anti-FLAG (1:200 dilution) and rabbit anti-myc (1:200 dilution) antibodies. *In situ* protein interactions were detected using the Duolink proximity ligation assay kit according to the manufacturer's instructions (Olink Bioscience). Cells were stained with BODIPY 493/503 and DAPI to visualize lipid droplets and nuclei, respectively. Confocal images were acquired using a Leica SP5 laser-scanning confocal microscope.

Oil Red O Staining—Cells were washed with PBS and then fixed with 4% paraformaldehyde in PBS for 30 min. After fixation, cells were washed with PBS followed by staining with 0.3% Oil Red 0 for 30 min. Cells were washed with 70% ethanol and then water. Images were captured with an Olympus 1X51 inverted microscope. After images were captured, TG content was quantified using ImageJ image analysis software to calculate the area stained with Oil Red O.

Statistical Analyses—Data are shown as mean ± standard deviation. Means were compared with a Tukey test or Student's *t* test. All experiments were performed at least three times unless otherwise indicated.

RESULTS

DGAT2 Is Part of a Large Protein Complex—We previously demonstrated that DGAT2 subunits interact with each other, suggesting that DGAT2 is part of a protein complex (9). To further characterize the nature of this DGAT2 complex, we treated membranes isolated from HEK-293T cells expressing FL-DGAT2 with the membrane permeable cross-linker, DSS. Immunoblotting with anti-FLAG showed that in the absence of cross-linker, a predominant 42 kDa band was present that represented the monomeric form of DGAT2 (Fig. 1*A*). When membrane samples were treated with DSS, high molecular weight immunoreactive material was observed (~650 kDa). As the concentration of DSS increased, there was a decrease in monomeric DGAT2 abundance with a corresponding increase in DGAT2 complex formation. We also noted a ~90 kDa band appearing at higher DSS concentrations that may represent a DGAT2 dimer.

To determine if DGAT2 formed a complex in intact cells and not just in isolated membrane fractions, HEK-293T cells expressing DGAT2 were treated with 500 μM DSS. Immunoblotting showed that in the absence of cross-linker, DGAT2 appeared as a 42 kDa monomer (Fig. 1*B*). As observed in isolated membranes (Fig. 1*A*), DGAT2 in intact cells exposed to DSS was also part of a large protein complex (Fig. 1*B*). Additionally, a ~90 kDa band was observed that corresponded to a DGAT2 dimer.

We hypothesized that DGAT2 is part of TG biosynthesis complex and that a lipogenic signal, such as incubation with oleate, might promote an increase in complex formation to increase TG synthesis. To test this, we examined DGAT2 complex abundance in HEK-293T cells expressing FL-DGAT2 that were treated with or without oleate and then cross-linked with DSS. We found that stimulating TG synthesis with oleate did not appear to increase DGAT2 oligomer abundance (Fig. 1*C*). Furthermore, DGAT2 oligomerization was not impaired when cells were deprived of fatty acids (data not shown).

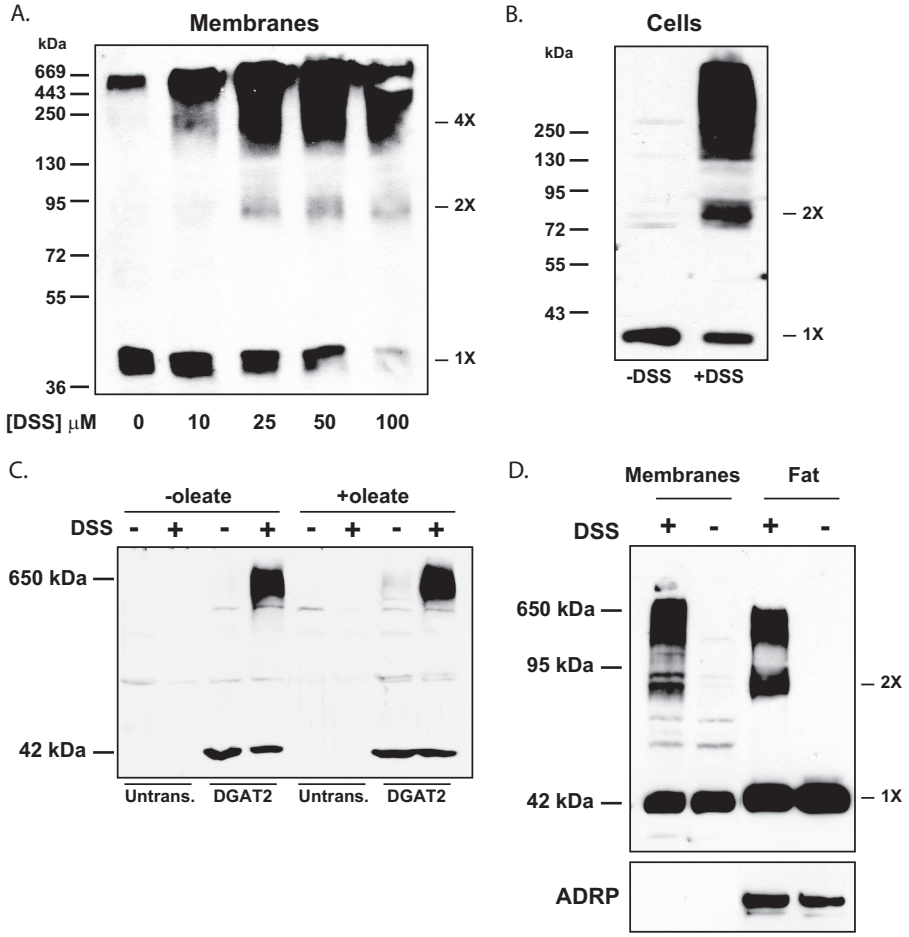

FIGURE 1. **DGAT2 is part of large ~650 kDa protein complex.** *A*, membranes from HEK-293T cells expressing FL-DGAT2 were exposed to DSS at the indicated concentrations. Samples were then immunoblotted with anti-FLAG. In the absence of DSS, DGAT2 was predominantly a ~42 kDa monomer. *1X*, monomer; *2X*, dimer; *4X*, possible tetramer. *B*, cross-linking of DGAT2 in intact cells. HEK-293T cells expressing FL-DGAT2 were treated with 500 μM DSS for 30 min. Membranes were then isolated by ultracentrifugation, separated by SDS-PAGE, and immunoblotted with anti-FLAG. *C*, oleate loading does not stimulate complex formation. HEK-293T cells expressing FL-DGAT2 were treated with or without 0.5 mM oleate for 12 h to stimulate lipid droplet formation followed by incubation with 500 μM DSS for 30 min. Membranes were isolated as previously described. Samples were separated by SDS-PAGE and immunoblotted with anti-FLAG. (*Untrans.*, untransfected HEK-293T cells). *D*, HEK-293T cells expressing FL-DGAT2 were treated with 0.5 mM oleate complexed to fatty acid free bovine serum albumen for 12 h followed by incubation with 500 μM DSS for 30 min. Membranes and floating fat layers were then isolated by ultracentrifugation. Equal volumes of membranes and fat were separated by SDS-PAGE and immunoblotted with anti-FLAG and anti-ADRP antibodies.

Since DGAT2 is localized to both ER membranes and lipid droplets, we determined if DGAT2 was part of a protein complex on lipid droplets as well as in membranes. Intact HEK-293T cells expressing DGAT2 were treated with DSS after lipid droplet formation was first stimulated with 0.5 mM oleate for 12 h. In the absence of cross-linker, only monomeric DGAT2 was detected in both the membrane and floating fat fractions (Fig. 1*D*). In the presence of DSS, DGAT2 in both membranes and lipid droplets was part of a high molecular weight complex (Fig. 1*D*). We also observed that there appeared to be more DGAT2 dimer in the fat fraction than in membranes (Fig. 1*D*).

MGAT2 Cross-linking—Recently, MGAT2 was shown to exist as both a homodimer and homotetramer and also interacted with DGAT1 (22). Consistent with these findings, we also found that human MGAT2 formed a dimer (~80 kDa) when membranes isolated from HEK-293T cells expressing FL-MGAT2 were cross-linked with DSS (Fig. 2). However, we did not observe a discrete tetramer, but instead saw much larger molecular weight material, similar to that observed for DGAT2

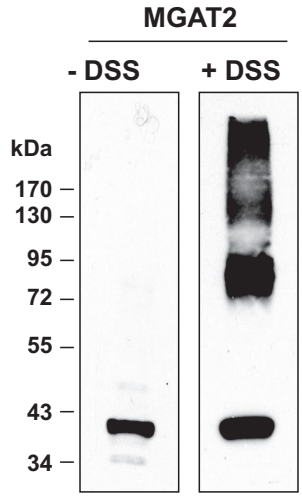

FIGURE 2. **Cross-linking of MGAT2 expressed in HEK-293T cells.** Membranes from HEK-293T cells expressing FL-MGAT2 were exposed to 100 μM DSS for 30 min. Samples were then immunoblotted with anti-FLAG.

(Fig. 1). In the absence of DSS, a single MGAT2 band was observed of ~38 kDa (Fig. 2).

MGAT2 Interacts with DGAT2—Stearoyl CoA desaturase (SCD)-1 and fatty acid transport protein (FATP)-1 are two enzymes that produce substrates (fatty acyl CoA) for DGAT enzymes and have been shown to interact with DGAT2 (23, 24). We sought to determine if DGAT2 interacts with the enzymes that produce 1,2-diacylglycerol, such as phosphatidate phosphatase/lipin and/or MGAT2. A recent study using chemical cross-linkers suggested that DGAT1, but not DGAT2, interacted with MGAT2 (22).

Since antibodies that detect endogenous DGAT2 in cells or tissues are not available, we co-expressed DGAT2 and MGAT2 in cells in culture and used co-immunoprecipitation experiments to determine if DGAT2 and MGAT2 interact. FL-MGAT2 and Myc-DGAT2 or untagged DGAT2 were transiently expressed together or separately in HEK-293T cells. Expression was confirmed by immunoblotting lysates of transfected cells with anti-FLAG and anti-DGAT2 antibodies (Fig. 3*A*). FL-MGAT2 was immunoprecipitated from detergent solubilized material with mouse anti-FLAG antibody (Fig. 3*A, lanes 8*, *10*, and *12*). When anti-FLAG immunoprecipitates were then immunoblotted with anti-DGAT2, Myc-DGAT2 and untagged DGAT2 could be detected only when co-expressed with FL-MGAT2 (Fig. 3*A, lanes 10* and *12*). No immunoreactive material was seen in untransfected cells or cells just expressing myc-DGAT2 or untagged DGAT2 (Fig. 3*A, lanes 7*, *9*, and *11*). We also could not detect the ER protein, PDI, or the mitochondrial protein, HSP70, in MGAT2 immunoprecipitates suggesting a specific interaction between DGAT2 and MGAT2 (Fig. 3*A*).

The interaction between MGAT2 and DGAT2 was verified by the reciprocal co-immunoprecipitation of DGAT2 and MGAT2 expressed in HEK-293T cells (Fig. 3*B*). FL-DGAT2 was immunoprecipitated with anti-FLAG and then the presence of myc-MGAT2 was determined by immunoblotting (Fig. 3*B*). Myc-MGAT2 was found only in immunoprecipitates when co-expressed with FL-DGAT2 (Fig. 3*B*).

We also examined if DGAT2 and DGAT1 interacted with lipin1. FL-lipin1 and Myc-DGAT1 or Myc-DGAT2 were co-expressed in HEK-293T cells. FL-lipin1 was immunoprecipitated from detergent solubilized material with mouse anti-FLAG antibody (Fig. 3*C*). The immunoprecipitates were then immunoblotted with anti-myc. After a lengthy exposure to film, a weak signal could be detected in the immunoprecipitates that corresponded to both DGAT1 and DGAT2 (Fig. 3*C*). This result suggests that either lipin1 may weakly interact with DGAT1, and DGAT2 or only a small fraction of the total cellular pool of lipin1 interacts with the DGAT enzymes.

In Situ Interaction of DGAT2 and MGAT2—To determine if DGAT2 and MGAT2 interacted in intact cells, we performed an *in situ* proximity ligation assay (25) on cells co-expressing FL-DGAT2 and myc-MGAT2. After oleate loading to stimulate lipid droplet formation, transfected cells were incubated with mouse anti-FLAG and rabbit anti-myc antibodies, followed by modified secondary antibody probes that will interact if they are in close proximity producing a red fluorescent signal. Lipid droplets were also stained with BODIPY 493/503 to identify DGAT2- and MGAT2-expressing cells and DAPI to visualize nuclei. When DGAT2 and MGAT2 were co-expressed, a red fluorescent interaction signal was detected, indicating that DGAT2 and MGAT2 were in close proximity to each other (< 40 nm) (Fig. 3*D*). In contrast, no red signal was detected in cells expressing only DGAT2 or MGAT2. These data confirm our co-immunoprecipitation experiments and provide additional evidence that DGAT2 and MGAT2 interact in intact cells.

Co-expression of DGAT2 and MGAT2 Stimulates TG Storage—We next examined TG accumulation in COS-7 cells expressing MGAT2, DGAT2, or MGAT2 and DGAT2 together that had been treated with 0.5 mM oleate for 12 h. Oil Red O staining of cells showed that expression of DGAT2, but not MGAT2, increased intracellular TG levels ~4-fold compared with control-transfected COS-7 cells (Fig. 4, *A* and *B*). When MGAT2 and DGAT2 were co-expressed TG levels were 1.4-fold higher than DGAT2-expressing cells and 5.5-fold higher than control-transfected cells, suggesting that MGAT2 is efficiently channeling DG to DGAT2 for TG synthesis (Fig. 4, *A* and *B*).

To identify the region of DGAT2 that interacted with MGAT2, we performed co-immunoprecipitation experiments with MGAT2 and various DGAT2 deletion mutants. Immunoblotting of inputs showed that MGAT2 and the DGAT2 mutants were expressed at similar levels (Fig. 4*C*). Deletion of two different N-terminal segments of DGAT2 had no detrimental effect on binding to MGAT2 (Fig. 4*C*). Also, a DGAT2 mutant containing only the N terminus and two transmembrane domains (Δ122–388) still interacted with MGAT2 (Fig. 4*C*). However, the interaction of MGAT2 with two DGAT2 mutants, both lacking the transmembrane domains (Δ1–119 and Δ66–115), was markedly reduced (Fig. 4*C*). The abundance of these two mutants in MGAT2 immunoprecipitates was much less when compared with DGAT2, suggesting that transmembrane domains of DGAT2 are important for its interaction with MGAT2.

An alternative explanation for the reduced interaction of these two mutants with MGAT2 is that they do not reside in the same subcellular compartment as MGAT2. The transmembrane domains of DGAT2 are required for targeting DGAT2 to the ER, and when they are removed, DGAT2 instead is localized to mitochondria (9). However, MGAT2 still interacted strongly with Δ122–388, which contains both transmembrane domains and is present in the ER, and two other N-terminal deletion mutants (Δ2–30 and Δ30–67) suggesting that the transmembrane domains are important for interacting with MGAT2 (Fig. 4*C*) (9).

We co-expressed MGAT2 and Δ66–115 in COS-7 cells to determine if disrupting the DGAT2/MGAT2 interaction had any functional consequence on TG storage. Although Δ66–115 is catalytically active, *in vitro* (9), co-expression with MGAT2 did not increase intracellular TG levels (Fig. 4, *A* and *B*). These findings suggested that a physical interaction between DGAT2 and MGAT2 is required to channel substrates for TG biosynthesis.

Co-localization of DGAT2 and MGAT2 at the ER—Since DGAT2 and MGAT2 interact they should be present in the same subcellular compartment. Consistent with previous stud-

ies, when expressed in COS-7 cells, immunofluorescence microscopy showed that both DGAT2 and MGAT2 were present in the ER (Fig. 5*A*) (10, 15). Furthermore, there was extensive co-localization of both DGAT2 and MGAT2 when their respective images were merged (Fig. 5*A*). DGAT2 is enriched in mitochondrial-associated membranes (MAM), which is a spe-

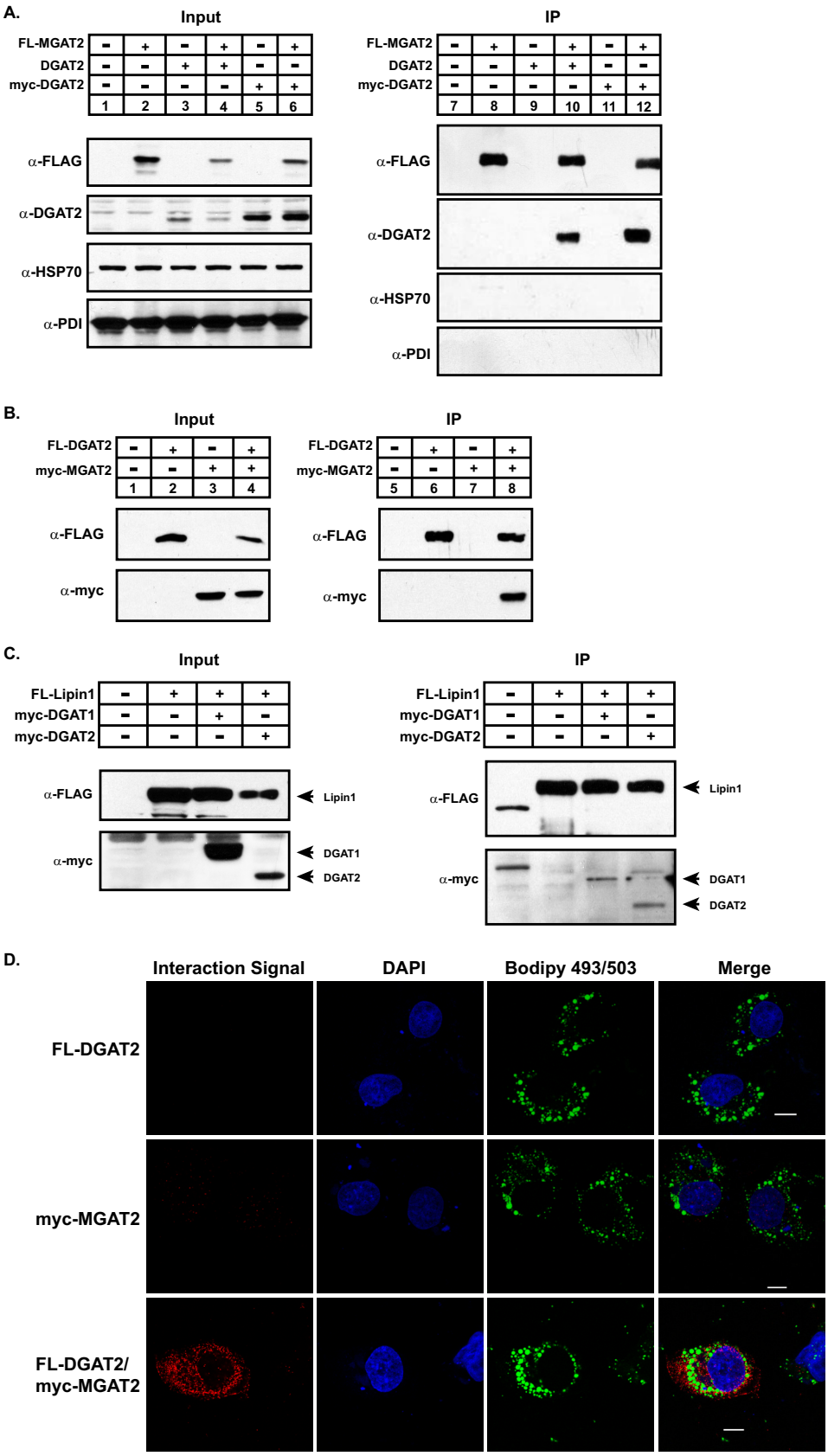

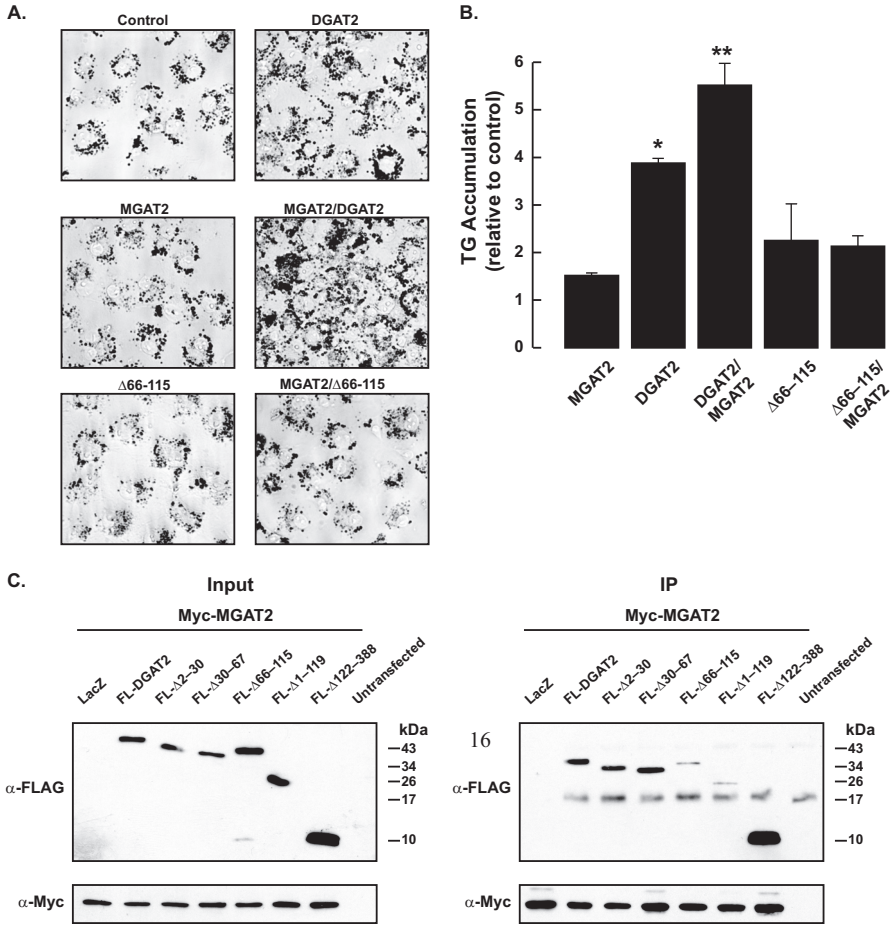

FIGURE 4. **Co-expression of MGAT2 and DGAT2 stimulates TG accumulation in intact cells.** *A*, accumulation of triacylglycerol as assessed by Oil Red O staining of COS-7-transfected cells. COS-7 cells expressing the indicated cDNAs were stimulated with 0.5 mM oleate for 12 h. Cells were fixed and then stained with Oil Red O to visualize triacylglycerol. *B*, triacylglycerol levels in Fig. 4*A* were quantified by measuring the area of Oil Red O staining. *, $p < 0.05$ compared with control-transfected cells. **, $p < 0.05$ compared with DGAT2-expressing cells. Data are from a representative experiment that was repeated twice. *C*, DGAT2 interacts with MGAT2 via its transmembrane domains. Myc-MGAT2 was co-expressed in HEK-293T cells with FL-DGAT2 or various DGAT2 deletion mutants. Myc-MGAT2 was immunoprecipitated with anti-myc agarose beads. Immunoprecipitates (*IP*) were then immunoblotted with anti-myc and anti-DGAT2 antibodies.

cialized region of the ER that is tightly bound to the outer mitochondrial membrane (10, 26, 27). We isolated microsomal and crude mitochondrial fractions, which contain both mitochondria and MAM from HEK-293T cells expressing either DGAT2 or MGAT2. We found that like DGAT2, MGAT2 is also enriched in the crude mitochondrial fraction, suggesting that it is also present in MAM along with DGAT2 (Fig. 5*B*).

MGAT2 Localizes to Lipid Droplets When Co-expressed with DGAT2—Consistent with previous reports, when expressed alone, DGAT2, but not MGAT2, becomes concentrated around the surface of lipid droplets when TG synthesis was stimulated by incubating cells with oleate (Fig. 6*A*) (9–11). Additionally, there was an increase in lipid droplet size with a corresponding decrease in number in DGAT2 expressing cells. In contrast, MGAT2 remained in the ER after incubation with oleate and did not appear to alter lipid droplet morphology (Fig. 6*A*). However, when co-expressed with DGAT2, oleate-loading resulted in the redistribution of both DGAT2 and MGAT2 to the surface of lipid droplets (Fig. 6*B*). Co-expression of lipin1, which is predominantly cytosolic, with DGAT2 did not cause lipin1 to redistribute to lipid droplets (Fig. 6*B*). Lipid droplets produced in cells co-expressing DGAT2 and MGAT2 were generally similar in size and number to those seen when DGAT2 was expressed alone. However, we also noticed a pop-

FIGURE 3. **Co-immunoprecipitation of DGAT2 and MGAT2 from HEK293T cells.** *A*, FL-MGAT2 was co-expressed with either myc-DGAT2 or untagged DGAT2 in HEK-293T cells. MGAT2 was immunoprecipitated with anti-FLAG agarose from detergent solubilized material. Immunoprecipitates (*IP*) were separated by SDS-PAGE and were then probed with anti-FLAG and anti-DGAT2. Immunoprecipitates were also probed with anti-PDI (Assay Designs) and anti-HSP70 (Thermo Scientific) antibodies as controls for nonspecific interactions. *B*, reciprocal co-immunoprecipitation of MGAT2 and DGAT2. FL-DGAT2 was co-expressed with myc-MGAT2 in HEK-293T cells. DGAT2 was immunoprecipitated with anti-FLAG-agarose from detergent solubilized material. Immunoprecipitates were separated by SDS-PAGE and were then probed with anti-FLAG and anti-myc antibodies. This experiment was repeated once with similar results. *C*, Lipin1 interacts weakly with both DGAT1 and DGAT2. FL-Lipin1 was co-expressed with either myc-DGAT1 or myc-DGAT2 in HEK-293T cells. FL-Lipin1 was immunoprecipitated with anti-FLAG agarose from detergent-solubilized material. Immunoprecipitates were separated by SDS-PAGE and were then probed with anti-myc. To visualize DGAT1 and DGAT2, PVDF membranes were exposed to film for extended periods of time. *D*, interaction of DGAT2 and MGAT2 was detected *in situ* using a proximity ligation assay. COS-7 cells expressing either FL-DGAT2, myc-MGAT2, or both together were stained with mouse anti-FLAG and rabbit anti-myc antibodies. Interaction signals (*red*) were detected using a Duolink detection kit. Nuclei were stained with DAPI (*blue*), and lipid droplets were stained with BODIPY 493/503 (*green*). Scale bar, 10 μM.

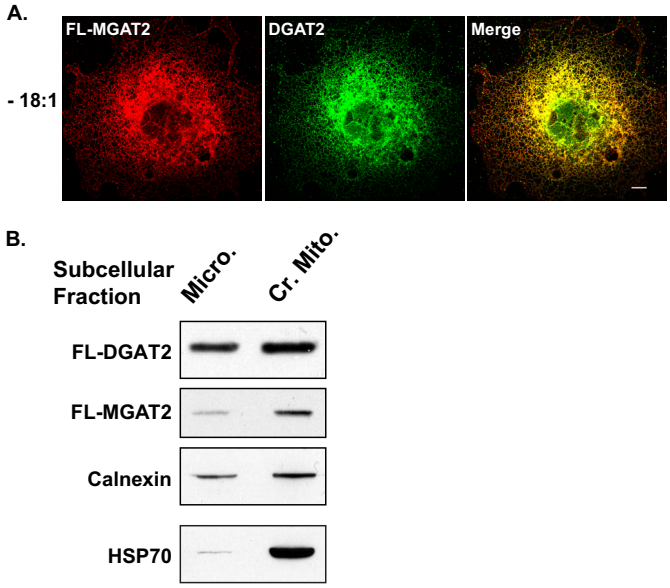

FIGURE 5. **MGAT2 and DGAT2 are present in the same subcellular compartment.** *A*, confocal immunofluorescence microscopy of FL-MGAT2 (*red*) and DGAT2 (*green*) transiently co-expressed in COS-7 cells. *B*, crude mitochondria (*Cr. Mito.*) and microsomes (*Micro.*) were isolated from HEK-293T cells expressing either FL-DGAT2 or FL-MGAT2. Equal amounts of protein from each fraction was separated by SDS-PAGE and immunoblotted with anti-FLAG, anti-calnexin, and anti-HSP70 antibodies.

ulation of many smaller lipid droplets not usually observed (Fig. 6*B*).

We also examined the subcellular distribution of DGAT2 and MGAT2 in membranes and lipid droplet fractions. Membranes and the floating fat layer containing lipid droplets were isolated from HEK293T cells expressing either FL-DGAT2, myc-MGAT2, or FL-DGAT2 and myc- MGAT2 together that had been treated with 0.5 mM oleate for 12 h. Immunoblotting showed that when cells were oleate-loaded, FL-DGAT2 was present in the fat layer as well as in the membrane fraction (Fig. 6*C*). In cells expressing only MGAT2, a small amount of MGAT2 protein could be detected in the lipid droplet fraction (Fig. 6*C*). However, consistent with our findings in Fig. 6*B*, MGAT2 was much more abundant in the lipid droplet fraction when co-expressed with DGAT2, suggesting that localization of MGAT2 to lipid droplets is dependent on its interaction with DGAT2 (Fig. 6*C*). Samples were also immunoblotted with anti-HSP70 and ADRP antibodies to assess the purity of the subcellular fractions (Fig. 6*C*). Less ADRP was present in the floating fat layer isolated from cells expressing only MGAT2 compared with cells expressing DGAT2. MGAT2 does not potently stimulate TG biosynthesis as well as DGAT2, which is reflected by decreased ADRP abundance.

2-Monoacylglycerol Stimulates Lipid Droplet Formation in McArdle RH7777 Cells—Typically, MGAT activity has been linked to the process of dietary fat absorption. However, Caco-2 cells, an enterocyte cell line routinely used to study this process, do not have a very active MGAT pathway and can be difficult to transfect (28). Furthermore, none of the known MGAT isoforms could be detected by Northern blotting mRNA isolated from Caco-2 cells, indicating that they are expressed at very low levels or not at all (29). Therefore, we chose to examine the functional importance of the DGAT2/MGAT2 interaction in

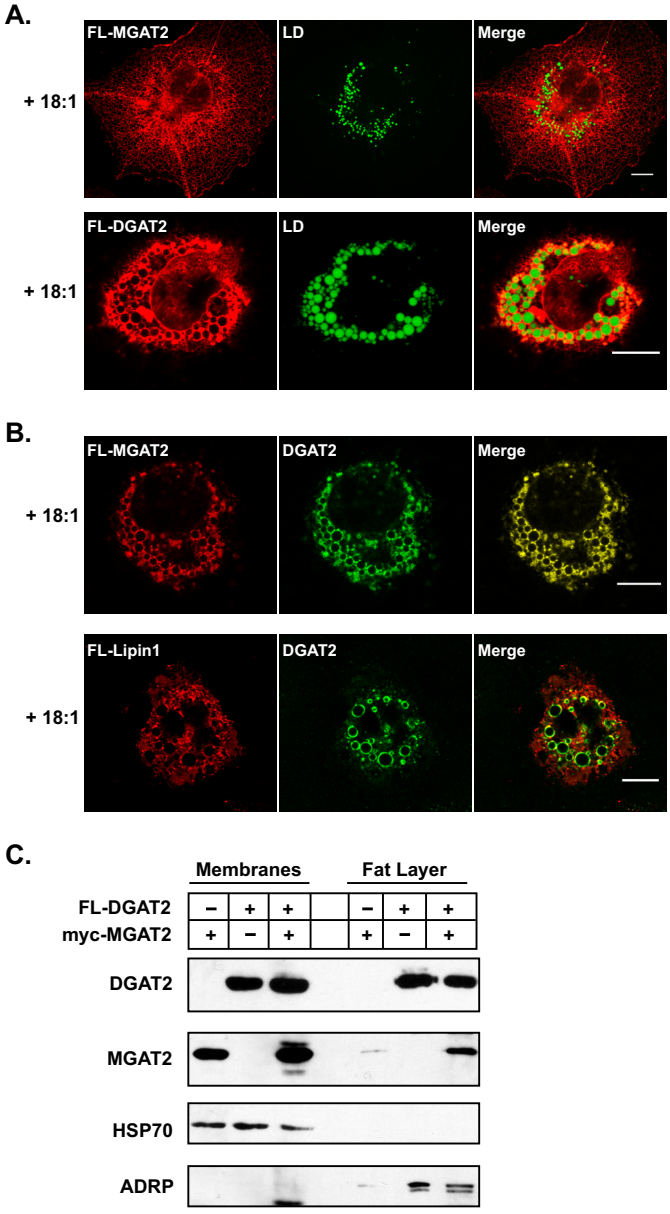

FIGURE 6. **MGAT2 interacts with lipid droplets in the presence of DGAT2 when expressed in COS-7 cells.** *A*, immunofluorescence microscopy of DGAT2 or MGAT2 expressed in COS-7 cells treated with 0.5 mM oleate for 12 h. DGAT2 and MGAT2 were stained with anti-FLAG and lipid droplets were visualized with BODIPY 493/503. *B*, COS-7 cells co-expressing DGAT2 and FL-MGAT2 or FL-lipin1 were incubated with 0.5 mM oleate for 12 h. DGAT2 was visualized with anti-rabbit DGAT2. FL-MGAT2 and FL-lipin1 were visualized with anti-mouse FLAG. Scale bar, 10 μM. *C*, HEK-293T cells co-expressing FL-DGAT2 and myc-MGAT2 were treated with 0.5 mM oleate for 12 h. Membranes and floating fat were isolated by ultracentrifugation. Equal volumes of membranes and fat were separated by SDS-PAGE and immunoblotted with anti-FLAG, anti-myc, anti-HSP70, and anti-ADRP antibodies.

McArdle RH7777 cells, a rat hepatoma cell line that has routinely been used as a model to study lipid metabolism in hepatocytes. Liver also has been shown to have significant levels of MGAT activity, *in vitro* (1, 30, 31). We confirmed that McArdle RH7777 cells also possessed MGAT activity by performing MGAT assays on cellular lysates. We found that when assayed in the absence of 2-monoacylglycerol, no MGAT activity could be detected (Fig. 7*A*). However, when exogenous 2-monoacylglycerol was included in the assay, MGAT activity was greatly

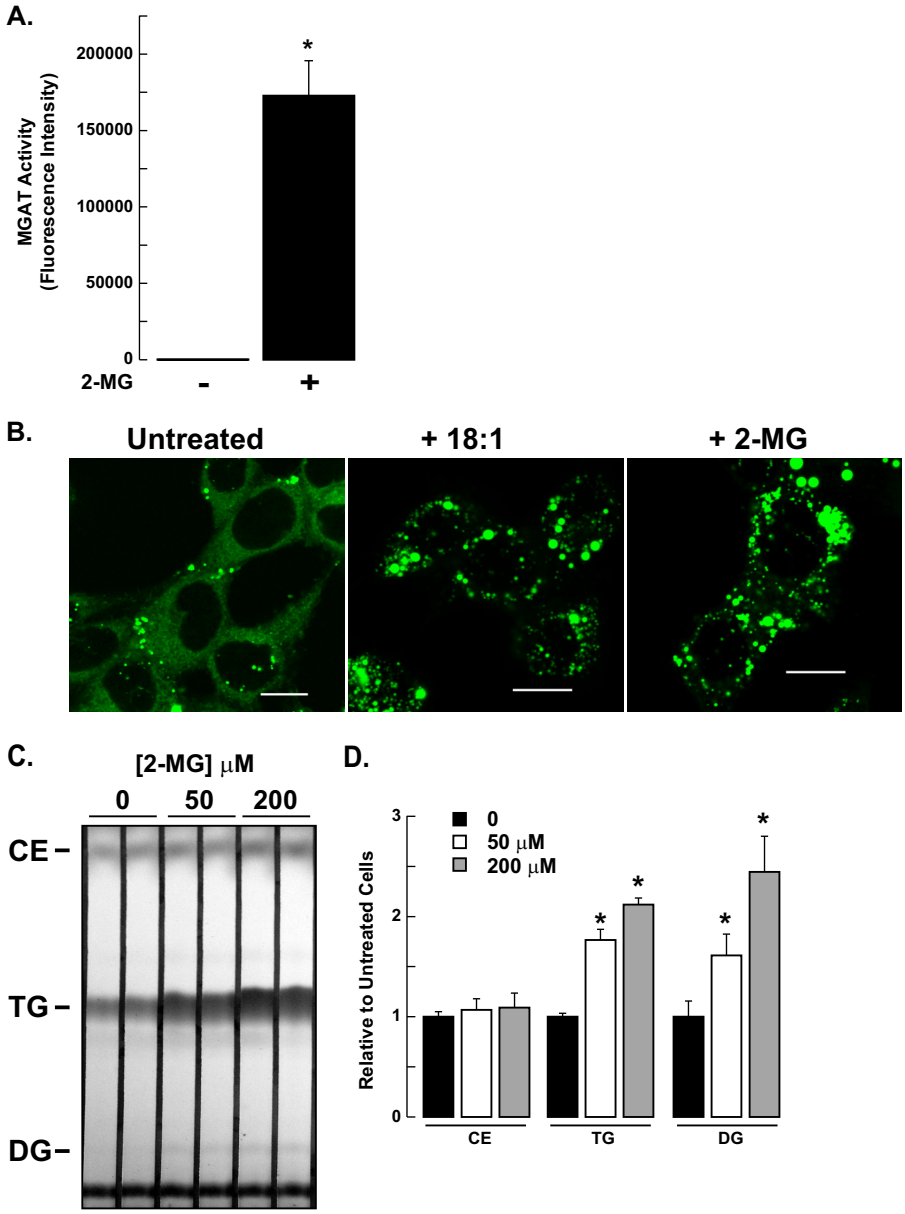

FIGURE 7. **2-monoacylglycerol can stimulate TG synthesis and cytosolic lipid droplet formation in McArdle RH7777 cells.** *A*, *in vitro* MGAT activity of McArdle RH7777 cells. Cell lysates were incubated with NBD-palmitoyl-CoA with or without monoacylglycerol (*2-MG*) as an acyl acceptor. *, $p < 0.05$ *versus* samples assayed without monoacylglycerol. Data are the average of two experiments performed in duplicate. *B*, McArdle RH7777 cells were incubated with or without 0.5 mM oleate or 0.2 mM 2-monoacylglycerol for 12 h. Lipid droplets were visualized with BODIPY 493/503. Scale bars: 10 μM. *C*, McArdle RH7777 cells were incubated with 50 or 200 μM 2-monoacylglycerol for 6 h, and lipids were extracted from equal amounts of cellular protein and separated by TLC. *D*, quantification of lipid levels in Fig. 6*C*, using Quantity One image analysis software (Bio-Rad). *, $p < 0.05$. Data are the average of two experiments performed in duplicate.

increased (Fig. 7*A*). MGAT2 may account for the majority of MGAT activity in McArdle cells as other MGAT isoforms have yet to be identified in rat liver (15, 31–33).

Lipid droplet formation in cultured cells is usually stimulated by incubating cells with fatty acids, such as oleate, which promotes the synthesis of TG that is stored in cytosolic lipids droplets. Addition of exogenous fatty acids increases substrate availability to the TG biosynthetic pathway. We sought to determine if 2-monoacylglycerol, one of the substrates of MGAT2, could also promote TG synthesis and lipid droplet formation in intact McArdle RH7777 cells. When McArdle rat hepatoma RH7777 cells were incubated with either 0.5 mM oleate or 0.2 mM 2-monoacylglycerol bound to albumen for 12 h, both lipid droplet number and size were increased relative to that of untreated cells (Fig. 7*B*).

To confirm that the increase in lipid droplets was due to the 2-monoacylglycerol being incorporated into diacylglycerol and subsequently TG, we analyzed the lipid composition of McArdle RH7777 cells treated with 0, 50 or 200 μM 2-monoacylglycerol for 6 h. Incubation of cells with either 50 or 200 μM 2-monoacylglycerol resulted in a visible increase in diacylglycerol levels compared with untreated cells (~2-fold) (Fig. 7, *C* and *D*). The TG content of 2-monoacylglycerol-treated cells also increased (~2-fold) compared with untreated cells while the amount of cholesterol ester remained unchanged (Fig. 7, *C* and *D*). Therefore, McArdle RH7777 cells are capable of utiliz-

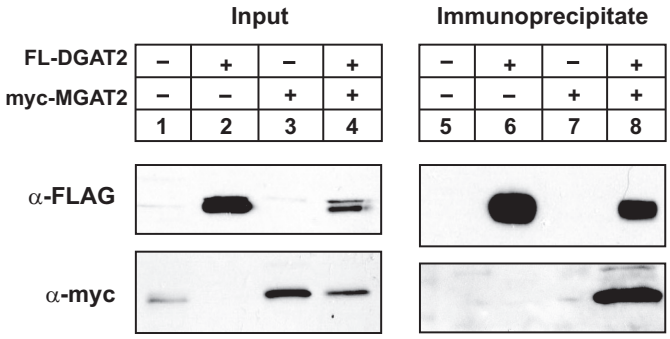

FIGURE 8. **Interaction of MGAT2 and DGAT2 in McArdle rat hepatoma RH7777 cells.** FL-DGAT2 was co-expressed with myc-MGAT2 in McArdle RH7777 cells. DGAT2 was immunoprecipitated with anti-FLAG agarose from detergent-solubilized material. Immunoprecipitates were separated by SDS-PAGE and were then probed with anti-FLAG and anti-myc antibodies to detect DGAT2 and MGAT2, respectively.

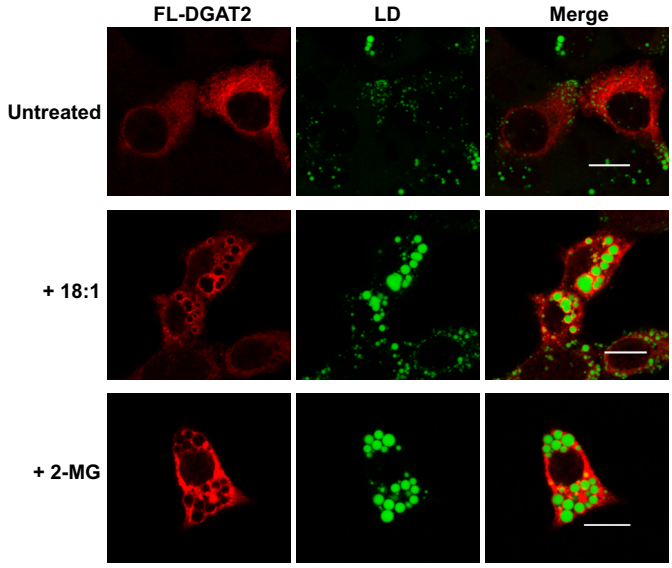

FIGURE 9. **DGAT2 associates with lipid droplets after stimulation of TG synthesis with monoacylglycerol.** McArdle RH7777 cells transiently expressing FL-DGAT2 were treated with either 0.5 mM oleate (18:1) or 2-monoacylglycerol (2-MG) complexed to fatty acid free bovine serum albumen for 12 h. DGAT2 was stained with anti-FLAG and lipid droplets (*LD*) were visualized with BODIPY 493/503. Scale bars: 10 μm.

ing 2-monoacylglycerol to produce diacylglycerol for TG biosynthesis via MGAT2.

MGAT2 and DGAT2 Interact in McArdle RH7777 Cells—We previously demonstrated that when expressed HEK-293T cells, DGAT2 and MGAT2 co-immunoprecipitated suggesting that they interact (Fig. 3). We performed a similar experiment in McArdle RH7777 cells that were transfected with either FL-DGAT2, myc-MGAT2, or both together. FL-DGAT2 was immunoprecipitated with anti-FLAG and then the presence of myc-MGAT2 was determined by immunoblotting (Fig. 8). As previously seen, Myc-MGAT2 was found only in immunoprecipitates when co-expressed with FL-DGAT2 (Fig. 8). This result indicates that the interaction between DGAT2 and MGAT2 is not unique to HEK-293T cells.

Monoacylglycerol Promotes the Association of DGAT2 with Lipid Droplets—Loading cells with oleate results in the redistribution of DGAT2, but not DGAT1, from the ER to lipid droplets (10, 11). To determine if 2-monoacylglycerol could also direct DGAT2 to lipid droplets from the ER, we incubated McArdle RH7777 cells transiently expressing FL-DGAT2 with oleate or 2-monoacylglycerol to stimulate TG synthesis, as described in Fig. 7. When McArdle RH7777 cells were incubated with oleate, DGAT2 became concentrated around large lipid droplets, compared with untreated cells, where DGAT2 remained in the ER (Fig. 9). Interestingly, incubation with 2-monoacylglycerol also resulted in the redistribution of DGAT2 from the ER to the lipid droplet surface (Fig. 9). These lipid droplets also had a similar morphology to those observed when TG synthesis was induced by oleate-loading, which are large droplets that are relatively few in number, compared with untreated cells (8). This result suggests that MGAT2 in McArdle RH7777 cells synthesizes diacylglycerol and channels it to DGAT2 for TG synthesis.

DISCUSSION

DGAT2 appears to be the major TG synthesizing enzyme in eukaryotic organisms. Mice lacking DGAT2 have almost no TG present (8). Overexpression of DGAT2 in cells in culture, mouse liver or skeletal muscle results in massive TG deposition in cytosolic lipid droplets (7, 8, 34, 35). Although DGAT2 is a potent DGAT enzyme, little is known about how it functions in cells to catalyze robust TG synthesis both at the ER membrane and in lipid droplets. In this study, we demonstrated that: 1) DGAT2 is part of a protein complex present in both membranes and lipid droplets, and 2) DGAT2 and MGAT2 can interact with each other to promote TG synthesis.

Almost all cellular processes require protein-protein interactions and it has been estimated that 80% of a cell proteome is part of a protein complex (36). Previous studies have suggested the existence of a TG biosynthesizing complex possessing distinct enzymatic activities needed for TG biosynthesis (37, 38). A protein complex was partially purified from rat intestine that contained DGAT, acyl CoA synthetase, acyl CoA acyltransferase and MGAT activities (37). This complex would have all of the necessary activities required to resynthesize dietary TG in enterocytes that are broken down to monoacylglycerol and fatty acids during the process of dietary fat absorption. A similar complex containing DGAT, acylglycerolphosphate acyltransferase, phosphatidic acid phosphatase and acyl carrier protein was identified in oleaginous yeast (38). However, at the time of these studies, the genes encoding the various proteins in these complexes were unknown.

Cross-linking experiments have shown that individual DGAT2 subunits are capable of interacting with each other (9). Furthermore, DGAT2 appears to be part of a large heterologous protein complex (>650 kDa) as co-immunoprecipitation experiments have shown that DGAT2 can interact with two proteins, FATP1 and SCD1 (9, 23, 24). Both of these enzymes catalyze the synthesis of substrates utilized by DGAT2 for TG synthesis. FATP1 possesses acyl CoA synthetase activity and activates fatty acids for DGAT2 (24, 39). SCD1 converts saturated fatty acyl CoAs to monounsaturated acyl CoAs which are abundant in TG (40). By interacting with DGAT2, both FATP1 and SCD1 could efficiently channel their respective substrates, which would facilitate TG synthesis.

Using co-immunoprecipitation, we have now identified MGAT2 as another DGAT2-interacting protein. Co-immunoprecipitation is a classic technique that has been routinely used to study protein-protein interactions (41, 42). Using this approach, we found that DGAT2 co-immunoprecipitated with MGAT2 both in HEK-293T and McArdle RH7777 cells. The immunoprecipitates were free of contaminating proteins, such as PDI and HSP70, suggesting that the interaction between MGAT2 and DGAT2 was specific. We confirmed these findings by performing *in situ* proximity ligation assays. This technique is a variation of immunofluorescence microscopy that can be used to determine if proteins interact in intact cells (25). A fluorescent signal is observed only when two proteins interact as they are in close proximity to each other (< 40 nm). Co-expression of MGAT2 and DGAT2 also resulted in higher intracellular TG levels than when DGAT2 was expressed alone, suggesting that these two enzymes work cooperatively to synthesize TG.

DGAT2 and MGAT2 were found to be present in the same subcellular compartments. Both enzymes co-localized in the ER and were enriched in MAM. Interestingly, MGAT2 was able to localize to lipid droplets when co-expressed with DGAT2. Previous studies have shown that MGAT2 expressed in COS-7 cells alone was not able to translocate to lipid droplets when cells were stimulated with fatty acids (10). Perhaps this is due to DGAT2 being expressed at low levels or not at all in COS-7 cells. Antibodies have failed to detect endogenous DGAT2 protein in this cell line. In contrast, MGAT2 has been detected in lipid droplets in murine enterocytes, where DGAT2 is highly expressed (1, 43).

In addition to its role in dietary fat absorption and chylomicron assembly in the intestine, we speculate that by binding to DGAT2, MGAT2 interacting with lipid droplets may generate the diacylglycerol needed to synthesize TG required for lipid droplet expansion. Analysis of the lipid composition of lipid droplets has shown significant amounts of diacylglycerol present, but the source has not been determined (11). Additionally, MGAT2 is highly expressed in adipose tissue in mice with only higher expression seen in small intestine and kidney (44). Since adipocytes do not have a role in TG secretion, it appears more likely that MGAT2 may participate in generating TG for storage in cytosolic lipid droplets in adipose tissue. This does not rule out that lipin1 is also a source of diacylglycerol for DGAT2. However, we were unable to localize lipin1 to lipid droplets. More likely, lipin1 synthesizes diacylglycerol at the ER for both phospholipid and TG synthesis.

Rodent liver has been shown to have a significant level of MGAT activity, *in vitro* (1, 15, 30, 31). MGAT2 is expressed at higher levels in human liver than in the small intestine and may be the only MGAT isoform expressed in rat liver (15). Therefore, MGAT2 may have an important yet underappreciated role in TG metabolism in this tissue. Incubating McArdle RH7777 cells, a rat liver hepatoma cell line, with 2-monoacylglycerol caused DGAT2 to become concentrated around large lipid droplets, analogous to what is observed when cells are incubated with oleate (10, 11). The exogenously added monoacylglycerol is most likely being used as a substrate by MGAT2 to generate diacylglycerol. The formation of large lipid droplets suggested that DGAT2, more so than DGAT1, is then utilizing MGAT2-derived diacylglycerol for TG synthesis. Additional, evidence in support of DGAT2 being able to utilize MGAT2-derived diacylglycerol comes from *Dgat1*-deficient mice. Mice lacking DGAT1 still absorb almost all dietary fat in the intestine, but at a reduced rate compared with wild-type mice (45). Therefore, DGAT2, which is expressed in the small intestine in mice, must be able to synthesize TG from diacylglycerol generated from MGAT2.

In a recent report, it has been shown that MGAT2 can interact with DGAT1, and that this interaction is dependent on an N-terminal region of DGAT1 (22). This study also reports that MGAT2 does not interact with DGAT2 (22). The evidence against an interaction between MGAT2 and DGAT2 was an apparent lack of heterodimer formation in cells co-expressing these two proteins. One explanation for this discrepancy is that the amount of DGAT2 protein expressed in cells was much lower than that of MGAT2 and was barely detectable by immunoblotting. Therefore, MGAT2 may preferentially form a homodimer, since the small amount of DGAT2 present would limit the amount of MGAT2/DGAT2 heterodimer formed. It is unlikely that any heterodimer would be detected even if 100% of DGAT2 protein were bound to MGAT2.

In conclusion, we have provided further evidence that DGAT2 interacts with other proteins to efficiently synthesize TG. The close proximity of FATP1, SCD1, and MGAT2 to DGAT2 would provide an efficient mechanism to provide the necessary substrates to DGAT2 for robust TG biosynthesis. This channeling of substrates may partially explain why DGAT2 is such a potent TG-synthesizing enzyme.

REFERENCES

1. Cases, S., Stone, S. J., Zhou, P., Yen, E., Tow, B., Lardizabal, K. D., Voelker, T., and Farese, R. V., Jr. (2001) Cloning of DGAT2, a second mammalian diacylglycerol acyltransferase, and related family members. *J. Biol. Chem.* **276,** 38870–38876
2. Kennedy, E. P. (1957) Metabolism of Lipides. *Annu. Rev. Biochem.* **26,** 119–148
3. Walther, T. C., and Farese, R. V. (2012) Lipid droplets and cellular lipid metabolism. *Annu. Rev. Biochem.* **81,** 687–714
4. Yen, C. L., Stone, S. J., Koliwad, S., Harris, C., and Farese, R. V., Jr. (2008) Thematic review series: glycerolipids. DGAT enzymes and triacylglycerol biosynthesis. *J. Lipid Res.* **49,** 2283–2301
5. Liu, Q., Siloto, R. M. P., Lehner, R., Stone, S. J., and Weselake, R. J. (2012) Acyl-CoA:diacylglycerol acyltransferase: Molecular biology, biochemistry and biotechnology. *Prog. Lipid Res.* **51,** 350–377
6. Stone, S. J., Levin, M. C., and Farese, R. V., Jr. (2006) Membrane topology and identification of key functional amino acid residues of murine acyl-CoA:diacylglycerol acyltransferase-2. *J. Biol. Chem.* **281,** 40273–40282
7. Monetti, M., Levin, M. C., Watt, M. J., Sajan, M. P., Marmor, S., Hubbard, B. K., Stevens, R. D., Bain, J. R., Newgard, C. B., Farese, R. V., Sr., Hevener, A. L., and Farese, R. V., Jr. (2007) Dissociation of hepatic steatosis and insulin resistance in mice overexpressing DGAT in the liver. *Cell Metab.* **6,** 69–78
8. Stone, S. J., Myers, H. M., Watkins, S. M., Brown, B. E., Feingold, K. R., Elias, P. M., and Farese, R. V., Jr. (2004) Lipopenia and skin barrier abnormalities in DGAT2-deficient mice. *J. Biol. Chem.* **279,** 11767–11776
9. McFie, P. J., Banman, S. L., Kary, S., and Stone, S. J. (2011) Murine diacylglycerol acyltransferase-2 (DGAT2) can catalyze triacylglycerol synthesis and promote lipid droplet formation independent of its localization to the endoplasmic reticulum. *J. Biol. Chem.* **286,** 28235–28246
10. Stone, S. J., Levin, M. C., Zhou, P., Han, J. Y., Walther, T. C., and Farese, R. V., Jr. (2009) The endoplasmic reticulum enzyme DGAT2 is found in

mitochondria-associated membranes and has a mitochondrial targeting signal that promotes its association with mitochondria. *J. Biol. Chem.* **284,** 5352–5361
11. Kuerschner, L., Moessinger, C., and Thiele, C. (2008) Imaging of lipid biosynthesis: how a neutral lipid enters lipid droplets. *Traffic.* **9,** 338–352
12. Han, G.-S., Wu, W.-I., and Carman, G. M. (2006) The Saccharomyces cerevisiae Lipin Homolog Is a Mg2+-dependent Phosphatidate Phosphatase Enzyme. *J. Biol. Chem.* **281,** 9210–9218
13. Reue, K., and Dwyer, J. R. (2009) Lipin proteins and metabolic homeostasis. *J. Lipid Res.* **50,** S109–S114
14. Yen, C. L., Cheong, M. L., Grueter, C., Zhou, P., Moriwaki, J., Wong, J. S., Hubbard, B., Marmor, S., and Farese, R. V., Jr. (2009) Deficiency of the intestinal enzyme acyl CoA:monoacylglycerol acyltransferase-2 protects mice from metabolic disorders induced by high-fat feeding. *Nat. Med.* **15,** 442–446
15. Yen, C. L., and Farese, R. V., Jr. (2003) MGAT2, a monoacylglycerol acyltransferase expressed in the small intestine. *J. Biol. Chem.* **278,** 18532–18537
16. Lehner, R., and Kuksis, A. (1996) Biosynthesis of triacylglycerols. *Prog. Lipid Res.* **35,** 169–201
17. Bell, R. M., and Coleman, R. A. (1980) Enzymes of glycerolipid synthesis in eukaryotes. *Annu. Rev. Biochem.* **49,** 459–487
18. Ho, S.-Y., Delgado, L., and Storch, J. (2002) Monoacylglycerol Metabolism in Human Intestinal Caco-2 Cells: Evidence for metabolic compartmentation and hydrolysis. *J. Biol. Chem.* **277,** 1816–1823
19. McFie, P. J., and Stone, S. J. (2011) A fluorescent assay to quantitatively measure in vitro Acyl CoA:Diacylglycerol acyltransferase activity. *J. Lipid Res.* **52,** 1760–1764
20. Bligh, E. G., and Dyer, W. J. (1959) A rapid method of total lipid extraction and purification. *Can. J. Biochem. Physiol.* **37,** 911–917
21. Peterson, T. R., Sengupta, S. S., Harris, T. E., Carmack, A. E., Kang, S. A., Balderas, E., Guertin, D. A., Madden, K. L., Carpenter, A. E., Finck, B. N., and Sabatini, D. M. (2011) mTOR Complex 1 Regulates Lipin 1 Localization to Control the SREBP Pathway. *Cell* **146,** 408–420
22. Zhang, J., Xu, D., Nie, J., Cao, J., Zhai, Y., Tong, D., and Shi, Y. (2014) Monoacylglycerol acyltransferase-2 is a tetrameric enzyme that selectively heterodimerizes with diacylglycerol acyltransferase-1. *J. Biol. Chem.* **289,** 10909–10918
23. Man, W. C., Miyazaki, M., Chu, K., and Ntambi, J. (2006) Colocalization of SCD1 and DGAT2: implying preference for endogenous monounsaturated fatty acids in triglyceride synthesis. *J. Lipid Res.* **47,** 1928–1939
24. Xu, N., Zhang, S. O., Cole, R. A., McKinney, S. A., Guo, F., Haas, J. T., Bobba, S., Farese, R. V., Jr., and Mak, H. Y. (2012) The FATP1–DGAT2 complex facilitates lipid droplet expansion at the ER–lipid droplet interface. *J. Cell Biol.* **198,** 895–911
25. Soderberg, O., Gullberg, M., Jarvius, M., Ridderstrale, K., Leuchowius, K.-J., Jarvius, J., Wester, K., Hydbring, P., Bahram, F., Larsson, L.-G., and Landegren, U. (2006) Direct observation of individual endogenous protein complexes *in situ* by proximity ligation. *Nat. Meth.* **3,** 995–1000
26. Cui, Z., Vance, J. E., Chen, M. H., Voelker, D. R., and Vance, D. E. (1993) Cloning and expression of a novel phosphatidylethanolamine *N*-methyltransferase. A specific biochemical and cytological marker for a unique membrane fraction in rat liver. *J. Biol. Chem.* **268,** 16655–16663
27. Rusiñol, A. E., Cui, Z., Chen, M. H., and Vance, J. E. (1994) A unique mitochondria-associated membrane fraction from rat liver has a high capacity for lipid synthesis and contains pre-Golgi secretory proteins including nascent lipoproteins. *J. Biol. Chem.* **269,** 27494–27502
28. Levy, E., Mehran, M., and Seidman, E. (1995) Caco-2 cells as a model for intestinal lipoprotein synthesis and secretion. *FASEB J.* **9,** 626–635
29. Cao, J., Hawkins, E., Brozinick, J., Liu, X., Zhang, H., Burn, P., and Shi, Y. (2004) A predominant role of acyl-CoA:monoacylglycerol acyltransferase-2 in dietary fat absorption implicated by tissue distribution, subcellular localization, and up-regulation by high fat diet. *J. Biol. Chem.* **279,** 18878–18886
30. Coleman, R. A., and Haynes, E. B. (1984) Hepatic monoacylglycerol acyltransferase. Characterization of an activity associated with the suckling period in rats. *J. Biol. Chem.* **259,** 8934–8938
31. Yen, C. L., Stone, S. J., Cases, S., Zhou, P., and Farese, R. V., Jr. (2002) Identification of a gene encoding MGAT1, a monoacylglycerol acyltransferase. *Proc. Natl. Acad. Sci. U.S.A.* **99,** 8512–8517
32. Cheng, D., Iqbal, J., Devenny, J., Chu, C.-H., Chen, L., Dong, J., Seethala, R., Keim, W. J., Azzara, A. V., Lawrence, R. M., Pelleymounter, M. A., and Hussain, M. M. (2008) Acylation of Acylglycerols by Acyl Coenzyme A:Diacylglycerol Acyltransferase 1 (DGAT1): Functional importance of DGAT1 in the intestinal fat absorption. *J. Biol. Chem.* **283,** 29802–29811
33. Cao, J., Cheng, L., and Shi, Y. (2007) Catalytic properties of MGAT3, a putative triacylgycerol synthase. *J. Lipid Res.* **48,** 583–591
34. Millar, J. S., Stone, S. J., Tietge, U. J., Tow, B., Billheimer, J. T., Wong, J. S., Hamilton, R. L., Farese, R. V., Jr., and Rader, D. J. (2006) Short-term overexpression of DGAT1 or DGAT2 increases hepatic triglyceride but not VLDL triglyceride or apoB production. *J. Lipid Res.* **47,** 2297–2305
35. Levin, M. C., Monetti, M., Watt, M. J., Sajan, M. P., Stevens, R. D., Bain, J. R., Newgard, C. B., Farese, R. V., Sr., and Farese, R. V., Jr. (2007) Increased lipid accumulation and insulin resistance in transgenic mice expressing DGAT2 in glycolytic (type II) muscle. *Am. J. Physiol. Endocrinol. Metab.* **293,** E1772–E1781
36. Berggård, T., Linse, S., James, P. (2007) Methods for the detection and analysis of protein-protein interactions. *Proteomics* **7,** 2833–2842
37. Lehner, R., and Kuksis, A. (1995) Triacylglycerol synthesis by purified triacylglycerol synthetase of rat intestinal mucosa. Role of acyl-CoA acyltransferase. *J. Biol. Chem.* **270,** 13630–13636
38. Gangar, A., Karande, A. A., and Rajasekharan, R. (2001) Isolation and Localization of a Cytosolic 10 S Triacylglycerol Biosynthetic Multienzyme Complex from Oleaginous Yeast. *J. Biol. Chem.* **276,** 10290–10298
39. Coe, N. R., Smith, A. J., Frohnert, B. I., Watkins, P. A., and Bernlohr, D. A. (1999) The Fatty Acid Transport Protein (FATP1) Is a Very Long Chain Acyl-CoA Synthetase. *J. Biol. Chem.* **274,** 36300–36304
40. Ntambi, J. M., and Miyazaki, M. (2004) Regulation of stearoyl-CoA desaturases and role in metabolism. *Prog. Lipid Res.* **43,** 91–104
41. Ren, L., Emery, D., Kaboord, B., Chang, E., and Qoronfleh, M. W. (2003) Improved immunomatrix methods to detect protein:protein interactions. *J. Biochem. Biophys. Methods* **57,** 143–157
42. Miernyk, J. A., and Thelen, J. J. (2008) Biochemical approaches for discovering protein–protein interactions. *Plant J.* **53,** 597–609
43. Seyer, A., Cantiello, M., Bertrand-Michel, J., Roques, V., Nauze, M., Bézirard, V., Collet, X., Touboul, D., Brunelle, A., and Coméra, C. (2013) Lipidomic and Spatio-Temporal Imaging of Fat by Mass Spectrometry in Mice Duodenum during Lipid Digestion. *PLoS ONE* **8,** e58224
44. Cao, J., Lockwood, J., Burn, P., and Shi, Y. (2003) Cloning and functional characterization of a mouse intestinal acyl-CoA:monoacylglycerol acyltransferase, MGAT2. *J. Biol. Chem.* **278,** 13860–13866
45. Buhman, K. K., Smith, S. J., Stone, S. J., Repa, J. J., Wong, J. S., Knapp, F. F., Jr., Burri, B. J., Hamilton, R. L., Abumrad, N. A., and Farese, R. V., Jr. (2002) DGAT1 is not essential for intestinal triacylglycerol absorption or chylomicron synthesis. *J. Biol. Chem.* **277,** 25474–25479